Charged clusters in strongly correlated electron gas

2003 J. Phys. A: Math. Gen. 36 9223

(http://iopscience.iop.org/0305-4470/36/35/309)

INSTITUTE OF PHYSICS PUBLISHING JOURNAL OF PHYSICS A: MATHEMATICAL AND GENERAL

J. Phys. A: Math. Gen. **36** (2003) 9223–9236 PII: S0305-4470(03)64018-7

Charged clusters in strongly correlated electron gas

M Saarela[1], **T Taipaleenmäki**[1] **and F V Kusmartsev**[2]

[1] Department of Physics/Theoretical Physics, University of Oulu, FIN-90014 University of Oulu, Finland
[2] University of Loughborough, Department of Physics, LE11 3TU, UK

E-mail: Mikko.Saarela@oulu.fi

Received 28 May 2003
Published 20 August 2003
Online at stacks.iop.org/JPhysA/36/9223

Abstract

We examine a mixture of electrons and holes in semiconductors. It is well known that in such a system the effective Coulomb interaction is perfectly screened at long distances, which leads to Mott's metal–insulator phase transition. We show that the screening is not monotonic and at intermediate ranges there are regions of over-screening, which at low densities become strong enough to destroy the homogeneous mixture by clustering charges. We suggest that this phenomenon is responsible for the broad density distribution of the electron–hole liquid and the condensed plasma phase in silicon suggested by Smith and Wolfe (1995 *Phys. Rev.* B **51** 7521). When the hole mass is set equal to the proton mass we can study properties of the metallic hydrogen and show that at high pressures there is a phase transition into a crystal phase of protons.

PACS numbers: 71.30.+h, 71.35.−y, 71.35.Ee

1. Introduction

In semiconductors irradiation of light creates electrons and holes. At low densities each electron is bound with a hole creating an exciton. This process gives rise to a gas of excitons. When the density increases above a critical value the system undergoes a first-order phase transition into the electron–hole liquid phase. The condensation of such a liquid was first predicted by Keldysh [1]. The key condition for its stability is the degeneracy of the electron and hole band structures, which lowers the Fermi kinetic energy of the system. The early photoluminescence measurements to determine the phase diagram of the electron–hole mixture were conducted in the indirect gap semiconductors germanium and silicon, which have highly degenerate energy bands [2–6]. Figure 1 shows the phase diagram in the uniaxially stressed silicon by Kulakovskii *et al* [7]. Later in a long series of carefully analysed measurements of the luminescence spectra in silicon Smith and Wolfe [8] suggested the existence of a third

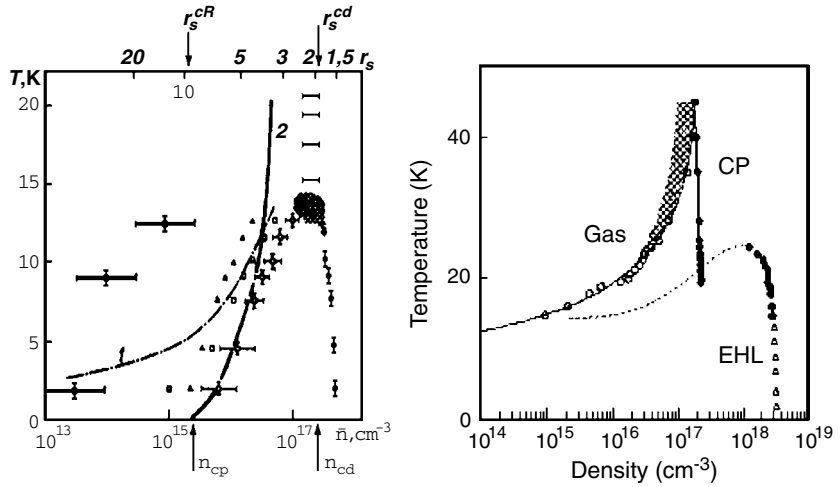

Figure 1. The left figure shows the gas–electron–hole liquid phase diagram of the uniaxially stressed silicon measured by Kulakovskii *et al* [7] in the temperature–density plane. Symbols • with experimental error bars mark the liquid phase. Curve 1 is the thermodynamic-equilibrium density of the exciton gas and curve 2 is the Mott-transition line. The right figure gives the phase diagram of the unstressed silicon measures and analysed by Smith and Wolfe [8]. The condensed plasma phase marked with (CP) is clearly shown.

phase, which they called a condensed plasma phase. It is also a liquid-like phase because the density remains roughly constant with increasing temperature. Figure 1 shows also their phase diagram in the temperature–density plane. Recently interesting measurements on direct gap semiconductors have been performed, which indicate that the electron–hole liquid is not homogeneous, but broken into droplets [9].

From the theoretical point of view the interesting issue in the electron–hole liquid is the screening of the Coulomb interaction. In a series of papers, Rice and his coworkers have analysed the band structures of a large number of semiconductors and calculated the exchange and correlation energies reaching a good agreement with experiments [10, 11]. The difficult exchange and correlation energy calculations were simplified by Vashishta and Kalia who derived a universal result which is independent of degeneracy and masses within the range of values typical in semiconductors [12].

In this work, we present the microscopic, variational many-body theory based on the Jastrow–Feenberg wavefunction which is very accurate in strongly correlated but dilute mixtures such as the ^{3}He–^{4}He mixture [13, 14]. The same method has been applied to the charged Bose gas [15]. Earlier simpler implementations were applied to positron annihilation and also to the electron–hole mixture [16–18]. The perfect screening of the Coulomb interaction at long distances is naturally embedded into this method, but as we shall see the screening is not monotonic. The attraction between two impurities induced by the many-body effects becomes at intermediate ranges stronger than the Coulomb repulsion and that creates regions of over-screening. At the critical density the attraction becomes strong enough to bind clusters of impurities indicating a phase transition into a mixture of charged clusters. The effects of this new phase of charged clusters on electron–hole liquid are the issue of this paper.

We will show first results on a negatively charged Bose gas, the bosonic electron gas, with one or two hole impurities embedded. The advantage of this system is that one can concentrate on the screening of the Coulomb interaction in the many-body system, separated

from the fermionic nature. When the electron and hole masses are equal we can simulate the annihilation of positrons into the electron gas. When the density is low enough one encounters Mott's metal–insulator transition. Estimates on the transition density are usually based on estimates of the range of the exponential screening. But interestingly we find that the perfect screening of the Coulomb interaction seen by bosonic electrons turns into an effective repulsion at intermediate ranges. Of course, the oscillatory behaviour of the screened interaction is well known for fermions due to the behaviour of the Lindhard function where the wavelength of those Friedel oscillations is $2k_F$. Similarly the Coulomb repulsion of two hole impurities is screened by the electron medium. Regions of over-screening appear, which bind two holes together at much higher density than the Mott-transition density.

A finite concentration mixture of charged bosons, however, is not a stable system because the compressibility of the charged Bose gas is negative and the pure system is stable only because the background jellium charge is fixed in position and not allowed to collapse. That is why the Fermi character of electrons and holes is essential for the stability of the mixture. Yet oscillations in the effective interaction between particles in the mixture due to the bosonic screening and Friedel oscillations make the clusterization possible and that is the new phase we predict here.

Finally, we let the hole mass in the mixture grow up to the proton mass and discuss properties of the liquid metallic hydrogen. We show that the liquid phase can exist only at high pressures and at lower pressure protons form a crystal.

2. Theory

The microscopic description of the electron–hole mixture begins with a well-defined Hamiltonian,

$$H = -\sum_{\alpha=e,h}\sum_{i=1}^{N_\alpha}\frac{\hbar^2}{2m_\alpha}\nabla_i^2 + \frac{1}{2}\sum_{\alpha,\beta=e,h}\sum_{i,j}{}'^{N_\alpha,N_\beta}\frac{q_\alpha q_\beta}{\varepsilon\left|\mathbf{r}_i^\alpha - \mathbf{r}_j^\beta\right|} \tag{1}$$

the Greek indices α and β refer to the type of a particle (electron or hole), and Latin subscripts i and j refer to the individual particles. The number of particles of each species is N_α, and $N = N_e + N_h$ is the total number of particles in the system. In terms of the concentration x of holes, we have

$$N_h = xN \qquad N_e = (1-x)N. \tag{2}$$

The prime on the summation symbol in equation (1) indicates that no two pairs (i,α), (j,β) can be the same. In semiconductors the masses are determined by the band structure and Coulomb forces between charges $q_e = -q_h = |e|$ are reduced by the dielectric constant ε. In the jellium model we add fictitious, uncorrelated background particles with infinite mass, which neutralize the charge. The required number of them is $N_b = |N_e - N_h|$ and their charge q_b is such that the total charge is zero, $N_b q_b + N_e q_e + N_h q_h = 0$. These localized background particles have no other structure or interaction with electrons or holes besides the Coulomb interaction.

It is customary to use excitonic units where energies are measured in units of the binding energy of the electron–hole pair, called excitonic Rydberg $E_x = \mu e^4/(2\hbar^2\varepsilon^2)$ with the reduced mass $\mu = m_e m_h/(m_e + m_h)$. The length unit is then $a_x = \hbar^2\varepsilon/(\mu e^2) = a_0 m_e \varepsilon/\mu$ in terms of the Bohr radius a_0. All distances are calculated in units of $r_0 = (3V/(4\pi N_e))^{1/3}$, the average distance between electrons in the volume V, and all momenta in units of r_0^{-1}. The ratio $r_s = r_0/a_x$ defines the usual dimensionless density parameter. The Fermi

momentum of electrons, $k_{Fe} = (3\pi^2\rho_e/\nu_e)^{1/3}$, depends on their density $\rho_e = N_e/V$ and the degeneracy ν_e of the conduction bands. Similarly we define the Fermi momentum of holes $k_{Fh} = (3\pi^2\rho_h/\nu_h)^{1/3}$, where ν_h is the degeneracy of the hole bands. We allow the hole concentration x to vary and thus $k_{Fh} = k_{Fe}[\nu_e x/(\nu_h(1-x))]^{1/3}$.

2.1. Euler equations for the electron–hole mixture

The Jastrow method [13, 19, 20] makes a variational ansatz for the ground-state wavefunction of the form

$$\Psi_0\big(\{\mathbf{r}_i^{(\alpha)}\}\big) = \mathrm{e}^{\frac{1}{2}U(\{\mathbf{r}_i^{(\alpha)}\})}\Phi\big(\{\mathbf{r}_i^{(\alpha)}\}\big) \qquad U\big(\{\mathbf{r}_i^{(\alpha)}\}\big) = \frac{1}{2!}\sum_{\alpha,\beta}\sum_{i,j}{}' u^{\alpha,\beta}(\mathbf{r}_i,\mathbf{r}_j). \tag{3}$$

Here the shorthand notation $\big(\{\mathbf{r}_i^{(\alpha)}\}\big)$ in the list of arguments refers to the full list $\big(\mathbf{r}_1^{(e)},\ldots,\mathbf{r}_{N_e}^{(e)},\mathbf{r}_1^{(h)},\ldots,\mathbf{r}_{N_h}^{(h)}\big)$, and $\Phi_0\big(\{\mathbf{r}_i^{(\alpha)}\}\big)$ is a product of Slater determinants of plane waves ensuring the required antisymmetry of the fermions. For bosons $\Phi\big(\{\mathbf{r}_i^{(\alpha)}\}\big) = 1$. In the pair correlation functions $u^{\alpha\beta}(\mathbf{r}_i,\mathbf{r}_j)$ the species superscripts determine the type of correlation. All these functions are determined from the variational principle [14] using the Euler equations

$$\frac{\delta E}{\delta u^{\alpha\beta}(\mathbf{r}_i,\mathbf{r}_j)} = 0 \tag{4}$$

where

$$E = \frac{\langle\Psi_0|H|\Psi_0\rangle}{\langle\Psi_0|\Psi_0\rangle} \tag{5}$$

is the variational energy expectation value.

The key ingredients of the theory are, along with the correlation functions and partial densities $\rho_\alpha = N_\alpha/V$, the radial-distribution functions $g^{\alpha\beta}(r)$ and static structure functions $S^{\alpha\beta}(k)$, which are Fourier transforms of the radial-distribution functions

$$S^{\alpha\beta}(k) = \delta_{\alpha\beta} + \sqrt{\rho_\alpha\rho_\beta}\int \mathrm{d}^3r[g^{\alpha\beta}(r)-1]\,\mathrm{e}^{\mathrm{i}\mathbf{k}\cdot\mathbf{r}}. \tag{6}$$

The Euler equations are more conveniently derived using the matrix notation for 2×2 matrices. For example, for the interacting and non-interacting static structure functions we use notation

$$\mathbf{S}(\mathbf{k}) \equiv \begin{pmatrix} S^{(ee)}(k) & S^{(eh)}(k) \\ S^{(eh)}(k) & S^{(hh)}(k)\end{pmatrix} \qquad \text{and} \qquad \mathbf{S_F}(\mathbf{k}) \equiv \begin{pmatrix} S_F^{(ee)}(k) & 0 \\ 0 & S_F^{(hh)}(k)\end{pmatrix} \tag{7}$$

where $S_F^{(\alpha\alpha)}(k)$ is the static structure function of the non-interacting Fermi gas of the component α

$$S_F^{(\alpha\alpha)}(k) = \begin{cases} \frac{3}{4}\frac{k}{k_{F\alpha}} - \frac{1}{16}\big(\frac{k}{k_{F\alpha}}\big)^3 & k \leqslant 2k_{F\alpha} \\ 1 & k \geqslant 2k_{F\alpha}. \end{cases} \tag{8}$$

The full set of Fermi hypernetted chain (FHNC) equations for the mixture is derived in [17]. We are, however, interested here in cases where a simplified version called a single loop approximation (FHNC//0) is applicable. This approximation sums self-consistently all chain and parallel-connected diagrams, but omits propagator corrections. At high densities the interaction effects in the electron gas become less important and the single loop approximation gives energies and structure functions in good agreement with Monte Carlo simulations. We expect that the same is true for the mixture also.

We present here only the main assumptions and results within the FHNC//0 approximation and refer to the original paper for details [14]. The HNC-equations connect the correlation functions to the direct distribution function

$$\Gamma^{\alpha\beta}(r) = \mathrm{e}^{u^{\alpha\beta}(r)+N^{\alpha\beta}(r)} \tag{9}$$

where the nodal sums $N^{\alpha\beta}(r)$ are solved from the Ornstein–Zernike equations in momentum space. These equations can be written in the matrix form in momentum space

$$\tilde{\mathbf{N}}(k) = \tilde{\Gamma}(k) - \tilde{\mathbf{X}}(k) \qquad \text{and} \qquad \tilde{\mathbf{N}}(k) = [\tilde{\mathbf{X}}\mathbf{S_F}\tilde{\Gamma}](k) \tag{10}$$

with a direct correlation function matrix $\tilde{\mathbf{X}}(k)$.

Within the single loop approximation the Fourier transform of $\Gamma^{\alpha\beta}(r)$ is connected to the structure function matrix

$$\mathbf{S}(k) = \mathbf{S_F}(k) + [\mathbf{S_F}\tilde{\Gamma}\mathbf{S_F}](k). \tag{11}$$

Without going into further details we assert that the coupled Euler equations (4) can be written in the form

$$[\mathbf{S}^{-1}\mathbf{H_1}\mathbf{S}^{-1}](k) - \left[\mathbf{S_F}^{-1}\mathbf{H_1}\mathbf{S_F}^{-1}\right](k) = 2\tilde{\mathbf{V}}_{p-h}(k). \tag{12}$$

The matrix $\mathbf{H_1}(k)$ has simply free particle kinetic energies in the diagonal and $\tilde{\mathbf{V}}_{p-h}(k)$ is the Fourier transform of the so-called particle–hole interaction,

$$V_{p-h}^{(\alpha\beta)}(r) = [1+\Gamma^{(\alpha\beta)}(r)]V_C^{(\alpha\beta)}(r) + \left[\frac{\hbar^2}{2m_\alpha} + \frac{\hbar^2}{2m_\beta}\right]\left|\nabla\sqrt{1+\Gamma^{(\alpha\beta)}(r)}\right|^2 + \Gamma^{(\alpha\beta)}(r)w_{\mathrm{I}}^{(\alpha\beta)}(r) \tag{13}$$

where $V_C^{(\alpha\beta)}(r)$ is the Coulomb interaction between particles α and β and $\tilde{\mathbf{w}}_{\mathrm{I}}(k)$ is the induced interaction matrix in momentum space,

$$\tilde{\mathbf{w}}_{\mathrm{I}}(k) = -\tilde{\mathbf{V}}_{p-h}(k) - \tfrac{1}{2}\left[\mathbf{S_F}^{-1}\mathbf{H_1}\tilde{\Gamma} + \tilde{\Gamma}\mathbf{H_1}{\mathbf{S_F}}^{-1}\right](k). \tag{14}$$

Equations (12), (13) and (14) form a closed set of equations that can be solved by iteration until convergence is reached. From these distribution and structure functions the variational total energy E can then be calculated.

The necessary condition for the existence of a solution to the Euler equation (12) is obtained by diagonalizing the Feynman-like matrix

$$\mathrm{diag}(\mathbf{H_1}\mathbf{S^{-1}}) = \mathbf{D}^{1/2} \tag{15}$$

and requiring this the eigenvalues are real. This is equivalent to the requirement that the eigenvalues of the matrix

$$\mathbf{H_1}\left[2\tilde{\mathbf{V}}_{p-h} + {\mathbf{S_F}}^{-1}\mathbf{H_1}{\mathbf{S_F}}^{-1}\right] \tag{16}$$

are positive definite. Diagonal elements of $\mathbf{D}^{1/2}$ are the Feynman approximations of the two collective excitations in the mixture; the optical and acoustic modes. In the exact theory these would be the exact energies of the collective modes in the long wavelength limit.

Let us return to the energetics of the mixture. At high densities and small values of r_s the dominating terms are the Fermi kinetic energy per electron

$$\frac{T_e}{N_e} = \frac{3}{5}\left(\frac{k_{Fe}^2}{2m_e} + \frac{x}{(1-x)}\frac{k_{Fh}^2}{2m_h}\right) \tag{17}$$

$$= \frac{3\gamma^2\mu}{5r_s^2}\left(\frac{1}{\nu_e^{2/3}m_e} + \frac{1}{\nu_h^{2/3}m_h}\left(\frac{x}{1-x}\right)^{5/3}\right) \tag{18}$$

where $\gamma = (9\pi/4)^{1/3}$, and the exchange energy of the non-interacting fermions,

$$\frac{E_{ex}}{N_e} = \sum_{\alpha=e,h} \frac{e^2}{\varepsilon} \int \frac{\mathrm{d}^3k}{(2\pi)^2} \frac{S_F^{\alpha\alpha}(k) - 1}{k^2} \tag{19}$$

$$= -\frac{3\gamma}{2\pi r_s} \left(\frac{1}{\nu_e^{1/3}} + \frac{1}{\nu_h^{1/3}} \left(\frac{x}{1-x} \right)^{4/3} \right). \tag{20}$$

The correlation energy is simplest to calculate using the coupling constant integration

$$\frac{E_c}{N_e} = \frac{1}{\pi \varepsilon r_s} \sum_{\alpha\beta} q_\alpha q_\beta \int_0^{r_s} \mathrm{d}\lambda \int_0^\infty \mathrm{d}k \left(S^{(\alpha\beta)}(\lambda, k) - S_F^{(\alpha\beta)}(k) \right) \tag{21}$$

and the main task is to evaluate the structure functions $S^{(\alpha\beta)}(\lambda, k)$ from the Euler equation (12) for different values of the density parameter λ ranging from zero to r_s.

2.2. One-component fluid and dilute mixture limit

The Euler equation which optimizes the one-component fluid is easily derived from equation (12) by ignoring the matrix nature of equations

$$S^{(ee)}(k) = \frac{S_F^{(ee)}(k)}{\sqrt{1 + \dfrac{4m_e \left[S_F^{(ee)}(k) \right]^2}{\hbar^2 k^2} \tilde{V}_{p-h}^{(ee)}(k)}} \tag{22}$$

and the bosonic fluid is obtained by setting $S_F^{(ee)} = 1$. In the coordinate space that becomes a Schrödinger-like equation for the radial-distribution function,

$$-\frac{\hbar^2}{m_e} \nabla^2 \sqrt{g^{(ee)}(r)} + \left[V_C^{(ee)}(r) + w_{\mathrm{I}}^{(ee)}(r) \right] \sqrt{g^{(ee)}(r)} = 0 \tag{23}$$

with the induced interaction written in the momentum space

$$\tilde{w}_{\mathrm{I}}^{(ee)}(k) = -\frac{[S^{(ee)}(k) - 1]^2}{2S^{(ee)}(k)} (2t_e(k) + \varepsilon_e(k)). \tag{24}$$

Here $t_\alpha(k) = \hbar^2 k^2/(2m_\alpha)$ is the free particle kinetic energy and $\varepsilon_e(k) = \hbar^2 k^2/(2m_e S^{(ee)}(k))$ is the Feynman energy for bosonic electrons. After solving these equations the variational energy of the system can be calculated using the coupling constant integration (21).

The single impurity limit is obtained from the mixture equations by setting $\Gamma^{(hh)}(r) = 0$ and $S_F^{(hh)}(k) = S^{(hh)}(k) = g^{(hh)}(r) = 1$. The Euler equation can be written in the form

$$S^{(eh)}(k) = -\frac{2\tilde{V}_{p-h}^{(eh)}(k) S^{(ee)}(k)}{t_h(k) + \varepsilon_e(k)}. \tag{25}$$

For the bosonic background particles this can again be written in the form of a Schrödinger-like equation

$$-\frac{\hbar^2}{2\mu} \nabla^2 \sqrt{g^{(eh)}(r)} + \left[V_C^{(eh)}(r) + w_{\mathrm{I}}^{(eh)}(r) \right] \sqrt{g^{(eh)}(r)} = 0 \tag{26}$$

with the reduced mass μ and the induced interaction

$$\tilde{w}_{\mathrm{I}}^{(eh)}(k) = -\frac{S^{(eh)}(k)(S^{(ee)}(k) - 1)}{2S^{(ee)}(k)} [t_e(k) + t_h(k) + \varepsilon_e(k)]. \tag{27}$$

This Euler equation minimizes the chemical potential of the impurity.

Charged impurities have two important properties which come out naturally from these equations. The first one is the perfect screening condition, which states that the induced interaction must screen the Coulomb interaction at long distances or equivalently at small k. Remembering that the Coulomb interaction dominates the particle–hole potential when k becomes small, $\tilde{V}^{(eh)}_{p-h}(k) \to \tilde{V}^{(eh)}_{C}(k)$ and using equation (14) we verify the screening property $\tilde{w}^{(eh)}_{I}(k) \to -\tilde{V}^{(eh)}_{C}(k)$. Inserting the limit into equation (25) we find that $S^{(eh)}(k=0) = 1$. The second condition is the cusp condition at $r = 0$, which is the result of the unscreened Coulomb interaction dominating the small r behaviour and the condition

$$-\frac{\hbar^2}{2\mu}\nabla^2\sqrt{g^{(eh)}(r)} + V^{(eh)}_{C}(r)\sqrt{g^{(eh)}(r)} = 0 \tag{28}$$

must be satisfied in the limit $r \to 0$, giving

$$\left.\frac{\mathrm{d}\log g^{(eh)}(r)}{\mathrm{d}r}\right|_{r=0} = -2r_s. \tag{29}$$

In the limit of two hole impurities we search for the solution of the (hh)-component of equation (12) after the background (ee)-component and the one-impurity (eh)-component are solved. We assume that the spins of the impurities are pointing to opposite directions and set $S^{(hh)}_{F} = 1$. Furthermore in the diagrammatic summations no intermediate particle can be a hole. This leads to a linear Schrödinger equation

$$\left[-\frac{\hbar^2}{m_h}\nabla^2 + V^{(hh)}_{\mathrm{eff}}(r) - E_b\right]\phi(\mathbf{r}) = 0 \tag{30}$$

where $V^{(hh)}_{\mathrm{eff}}(r) = V^{(hh)}_{C}(r) + w^{(hh)}_{\mathrm{I}}(r)$ is a local, effective interaction with the Fourier transform of the induced interaction

$$\tilde{w}^{(hh)}_{\mathrm{I}}(k) = -\frac{[S^{(eh)}(k)]^2}{2S^{(ee)}(k)}[2t_h(k) + \varepsilon_e(k)]. \tag{31}$$

Only the zero energy solution $E_b = 0$ is consistent with a homogeneous mixture equation and for $E_b < 0$ the mixture is unstable against pairing. Between two charged impurities the Coulomb interaction is again perfectly screened by the induced potential at long distances.

3. Results

We begin the study of the electron–hole mixtures by demonstrating the importance of the over-screened Coulomb interaction for the binding of the electron–hole pair known as the Mott metal–insulator transition. This occurs for the bosonic electrons at about $r_s \approx 6.5$ in excitonic units and at $r_s \approx 5.3$ for the fermionic electrons. But, already at much higher density, $r_s < 2$, another transition takes place where two holes form a bound pair due to the fact that electrons over-screen the Coulomb repulsion between them and create a range of attraction deep enough for binding.

The pure bosonic charged gas within the jellium model using the variational method has been carefully analysed [15] and is in excellent agreement with Monte Carlo simulations. If we set the impurity mass $m_h = m_e$, the system corresponds to a positron impurity in a bosonic electron fluid. The positive impurity collects around it a screening cloud and the distribution of electrons is given by the radial-distribution function $g^{(eh)}(r)$ solved from the Euler equation (26). The effective interaction which electrons feel around the impurity in the Schrödinger-like Euler equation is shown in figure 2. At short ranges the $1/r$ Coulomb attraction dominates, but at about $r \approx 1r_s a_x$ a repulsive region develops with decreasing

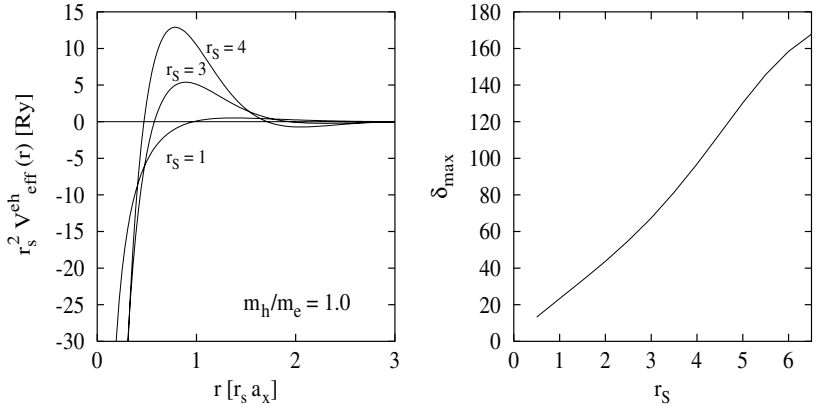

Figure 2. In the left figure are the effective potentials for one impurity in units of excitonic Rydbergs times r_s^2 for those r_s-values indicated in the figure. In the right figure is the maximum of the s-wave scattering phase-shift from the effective potential as a function of r_s.

density. At the same time the kinetic energy term in equation (26) diminishes like $1/r_s^2$. In the figure the effective potential is multiplied by that factor. From the effective potential we calculate the s-wave scattering phase shift and show that its maximum increases up to π as a function r_s, which tells that an electron cluster becomes bound around the impurity when $r_s \geqslant 6.5$. The exact limit is very difficult to reach numerically, because the effective potential is determined iteratively. That is why we have to rely on extrapolation of the results from $r_s \leqslant 6$.

The height of the peak of the radial-distribution function, $g^{(eh)}(r)$ increases rapidly and its width becomes narrower as a function of r_s. At the same time the structure function $S^{(eh)}(k)$ develops a large peak at about $k = 3/r_0$. The normalization sets $g^{(eh)}(\infty) = 1$ and the perfect screening condition requires that $S^{(eh)}(0) = 1$. From the height of the peak we can calculate the positron annihilation rate at contact $\lambda = \frac{12}{r_s^3} g^{(eh)}(r = 0) 10^{-9} \frac{1}{s}$. The results are shown in figure 3 in comparison with measurements. The agreement is surprisingly good for bosonic electrons. These results underline the importance of the Coulomb interaction and the exact conditions like the cusp and perfect screening conditions derived from it. The power of these conditions can be easily demonstrated by making the simplest parametrization

$$g^{(eh)}(r) - 1 = a\,\mathrm{e}^{-br} \tag{32}$$

and determining the parameters a and b in such a way that they are satisfied. The result is also shown in figure 3 and fits perfectly well the whole metallic region. Deviations from the Bose gas results begin from the region where the peak of the structure function or the dip in $g^{(eh)}(r)$ begins to grow faster than r_s^3, because the simple parametrization does not allow for a bound state formation which is evident at low densities. Figure 3 also shows a good agreement of our results for the correlation energy with the full fermionic calculations [23] up to $r_s = 3$, but above that we find a rapid decrease of the correlation energy consistent with the approaching binding of the electron cluster around the impurity.

The effective interaction between two hole impurities $V_{\mathrm{eff}}^{(hh)}(r)$ defined in equation (30) can be readily calculated after the impurity structure function $S^{(eh)}(k)$ is known. It has the $1/r$ repulsion at short distances and the perfect screening makes it short ranged, yet the screening is not monotonic and there are regions of over-screening. The results for equal masses $m_e = m_h$ are shown for different r_s-values in figure 4. They clearly demonstrate that the induced interaction over-screens the Coulomb repulsion and the attraction grows as a function of r_s.

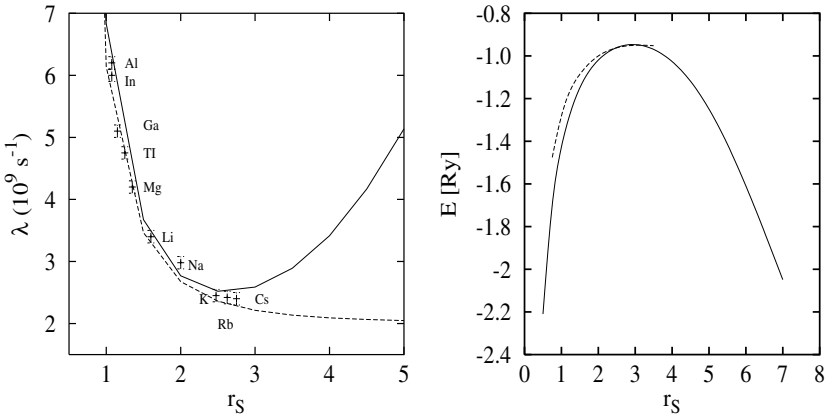

Figure 3. In the left figure are the annihilation rates as a function of r_s. The labelled experimental results are taken from [21, 22]. The solid line is our result for the positron annihilation into the charged Bose gas. The dashed line is the result of the simple approximation of equation (32). In the right figure are the correlation energies of the impurity from the present work for the charged Bose gas (solid curve). This is compared with the results of [23] for the correlation energy of the positron impurity in the electron gas (dashed curve).

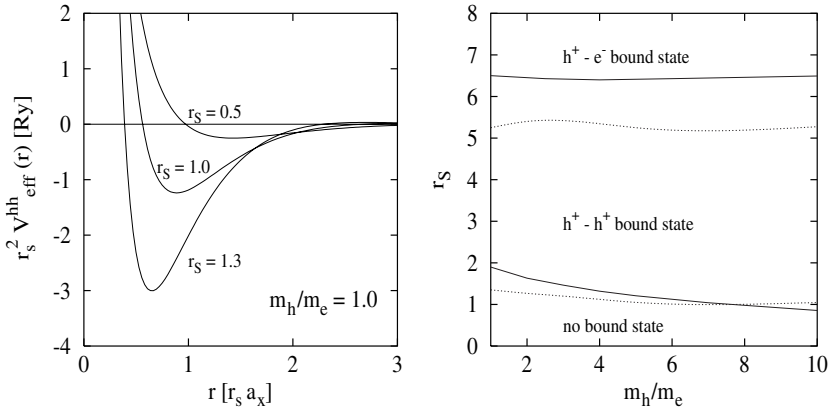

Figure 4. In the left figure we show the effective interaction between positive impurities in the bosonic electron gas for the impurity mass $m_h = m_e$ at r_s-values marked in the figure. On the right is the phase diagram of hole impurities in the bosonic electron gas (solid curves). For comparison we show also instability lines for impurities in the fermionic electron gas (dotted curves).

Already at $r_s > 2$ the potential can support a bound state. In figure 4 on the right we have collected the phase diagram for one and two impurities in the density–mass plane. The critical value $r_s^M \approx 6.5$ for the Mott transition is quite independent of the mass ratio m_h/m_e and the critical value $1 \leqslant r_s^P \leqslant 2$ for pairing decreases slightly when the mass ratio increases. The set of dashed curves in the figure gives the results where the fermionic character of electrons is included. Critical densities are then shifted to slightly higher densities in both cases.

The full mixture of charged particles cannot phase separate globally, because the charge must be neutralized. Yet, the mixture of charged bosons cannot be stable for any mass ratios or finite concentrations. This is seen by studying the Feynman-like excitation modes from equation (15). The two elementary modes are the plasmon and the sound mode, but the

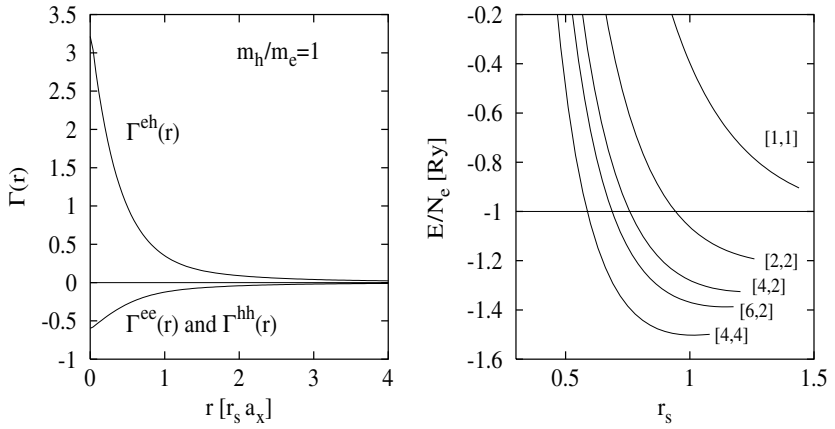

Figure 5. In the left figure we show the direct distribution functions $\Gamma^{(\alpha\beta)}(r)$ for the electron–hole mixture at $r_s = 1$. We assume that the electron and hole masses are equal. On the right is the total energy/electron of the mixture as a function of r_s for different valence and conduction band degeneracies, using $m_h = m_e$.

sound mode cannot be stable if the structure functions satisfy the Euler equation (12). This is because the compressibility of the charged Bose gas is always negative [15] and the only way this system remains stable is that the background jellium charge is not allowed to collapse. In the mixture both positive and negative particles are mobile and nothing prevents them from increasing the density. Thus the fermionic nature of electrons and holes is essential for a stable charged mixture.

Experimentally a mixture of electrons and holes can be created in semiconductors and semi-metals. It is unstable against annihilation, but if the annihilation rate is slow enough then the mixture can reach a thermodynamic equilibrium and condensate into the liquid phase. For a review of theories we refer to the articles by Rice *et al* [10, 11]. Here we present results from the variational calculations where we search for the stability limits of the zero temperature mixture by varying the density, mass ratio and degeneracy.

We begin by solving the Euler equations (12) for the mixture when $m_h = m_e$. The results for the direct distribution functions $\Gamma^{(\alpha\beta)}(r)$ are shown in figure 5 at the density $r_s = 1$. When the concentration of electrons and holes is equal then $\Gamma^{(ee)}(r) = \Gamma^{(hh)}(r)$ and they differ only when concentrations differ. $\Gamma^{(eh)}(r)$ displays the attraction between electrons and holes and the height of the peak increases with r_s as in the case of a single hole impurity.

In semiconductors the degeneracy of the band structure is essential for the binding of the electron–hole liquid. The minimum value of the sum of the kinetic and exchange energies for non-interacting fermions is independent of the degeneracy, but the location is shifted towards lower r_s-values, whereas the correlation energy is almost independent of the degeneracy [12]. This means that the higher the degeneracy the lower the energy per electron becomes. In figure 5 we show the total energy per electron of the electron–hole liquid as a function of r_s for different degeneracies. When there is only a single conduction and valence band, there is no minimum in the energy, but as the degeneracy raises a minimum in the energy appears. This minimum is below the exciton binding energy and that makes the electron–hole liquid stable against liquid–gas transition.

In figure 6 we show the energy per electron for Si, which has six degenerate electron bands and two degenerate hole bands. The anisotropy of the electron bands has been included

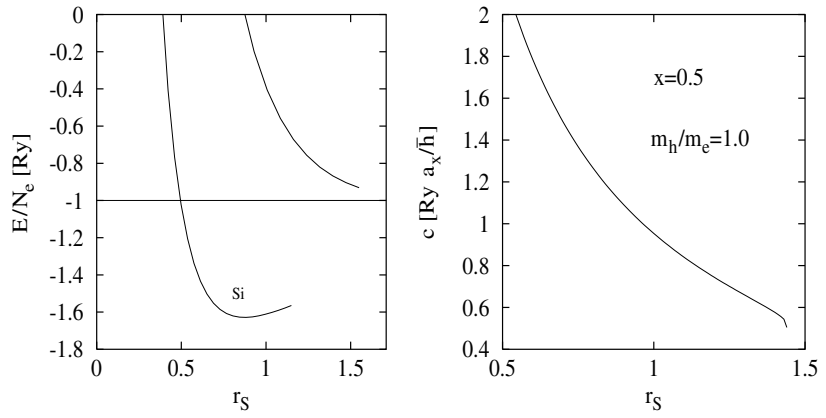

Figure 6. In the left figure is the energy/electron of the electron–hole mixture in silicon. For comparison we show the energy of a model system where the band structure is non-degenerate and $m_h = m_e$. In the right figure is the speed of sound of the acoustic mode as a function r_s of this model system.

in our calculation of the structure function $S_F^{(ee)}(k)$ and the difference in the effective hole masses is included in the Hartree–Fock energy following the method used by Combescot and Nozieres [24]. For the mass of the electron we use the values $m_{||} = 0.9163$ and $m_\perp = 0.1905$ and the masses of the heavy and light holes are $m_H = 0.523$ and $m_L = 0.154$, respectively. Since the correlation energy is fairly independent of the masses we can safely use there the spherical approximation for electrons

$$m_e = 3\left(\frac{1}{m_{||}} + \frac{2}{m_\perp}\right)^{-1} \tag{33}$$

and the average of the inverse masses of holes

$$m_h = 2\left(\frac{1}{m_H} + \frac{1}{m_L}\right)^{-1}. \tag{34}$$

We find the energy minimum at $r_s = 0.89$ with $E/N_e = -1.61$Ry. This agrees very well with experiments as well as with the calculation of Brinkman and Rice [10] who found the energy minimum $E/N_e = -1.59$Ry at $r_s = 0.84$.

All these energy curves show a termination point when $1.1 < r_s < 1.5$ depending somewhat on the degeneracy. This is the density where the mixture becomes unstable against cluster formation. We see this by calculating the speed of sound of the acoustic excitation mode. A typical case for equal electron and hole masses and with no degeneracy is shown in figure 6 on the right. At $r_s \approx 1.44$ the speed of sound begins to drop very rapidly and no stable solution for the mixture can be found. It indicates that the phase transition into a clustered phase is a first-order phase transition.

Finally, in figure 7 we show the phase diagram of the electron–hole mixture in the density–mass plane. When density is high enough a homogeneous metallic liquid exists for all mass ratios. Yet without the band degeneracies that can exist only under pressure and at zero pressure the mixture breaks into a liquid of charged clusters, which is a new kind of a phase. By varying the concentration of holes one can follow how the two-hole bound state instability also shown in figure 7 evolves into the clustering instability of the full mixture. We have not calculated the energetics of the clustered phase, but since the energy of the mixture at the instability is well below the free exciton energy in Si the new phase must be a low density

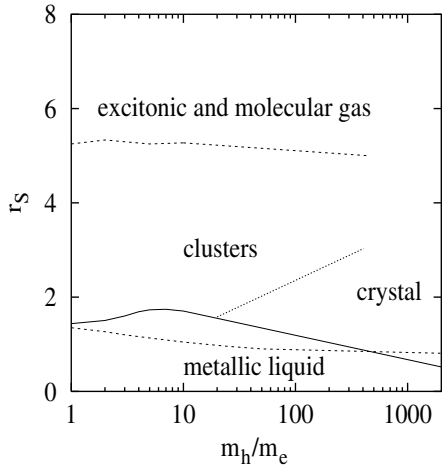

Figure 7. The phase diagram of the electron–hole mixture in the density–mass plane in excitonic units. The solid curve gives the critical density at which the homogeneous mixture with equal number of electrons and holes becomes unstable. For comparison we show the dilute hole concentration results for the Mott transition (upper dashed line) and bound pair formation (lower dashed line).

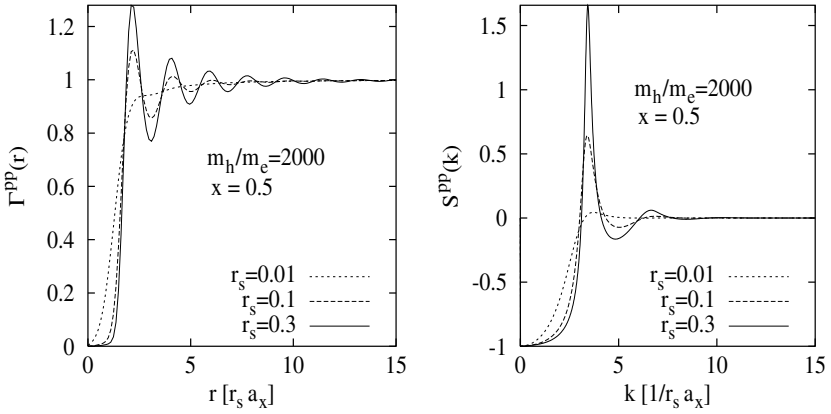

Figure 8. The proton–proton components $\Gamma^{pp}(r)$ and $S^{pp}(k)$ in the liquid metallic hydrogen for densities marked in the figure. Increasing oscillations in $\Gamma^{pp}(r)$ and increasing height of the peak in $S^{pp}(k)$ indicate that the density is approaching a solidification instability.

liquid. It could be a fairly shallow minimum where the cluster size is not uniform. This could be the phase analysed in the Wolfe and Smith experiment [8], which they call the condensed plasma phase. In the uniaxial stressed silicon experiments [7] show a very broad luminescence spectrum coming from the liquid phase. Since the stressing reduces the degeneracy and raises the energy minimum of the homogeneous mixture we expect that the new clustered phase gives a partial contribution to the luminescence spectrum and makes it broad. More recently reflectivity experiments on a direct gap semiconductor CuCl [9] have indicated inhomogeneity in the electron–hole liquid phase, which could be due to this new cluster phase.

In a more extreme case when we let the mass ratio m_h/m_e grow up to 2000 we reach the regime of the liquid metallic hydrogen. As seen from the phase diagram in figure 7 this system is at high densities in the homogeneous metallic phase. The instability reached by decreasing

the density does not break the system into clusters, instead we find that the new phase is a crystal of protons. The direct correlation function $\Gamma^{pp}(r)$ and structure function $S^{pp}(k)$ of the proton–proton component are shown in figure 8 for three densities in the approach to the instability. They clearly indicate a formation of an ordered phase. From the position of the peak of the structure function we can read the reciprocal lattice constant $k_r \approx 4/(r_s a_x)$. From the energetics we can also determine that the liquid metallic hydrogen can exist only at very high pressures before it turns into metallic atomic crystal. From this work, we cannot determine the metal–insulator transition density into the molecular H_2 crystal, which is the ground state of the electron–proton mixture at zero pressure and zero temperature. In the phase diagram we give only a rough estimate that if $m_h/m_e \geqslant 20$ then the transition from the homogeneous liquid into solid instead of clustered liquid will take place. At large mass ratios the atomic solid may then turn into molecular solid.

4. Summary

From our results we have concluded that many-body effects on screening of the Coulomb interaction lead to regions of over-screening which will bind two hole impurities and cluster electrons and holes in the full mixture of equal number of particles. The phase transition into this new clustered phase is of the first order and occurs at much higher density than Mott's metal–insulator transition. We have suggested that this phase would give new insight into the analysis of the luminescence spectra in semiconductors and recent reflectivity measurements on direct gap semiconductors.

Within the same theoretical framework we show that the liquid metallic hydrogen can exist only at high pressures before protons solidify into atomic metallic phase.

Acknowledgments

The work was supported, in part, by the Academy of Finland under project 100487 and the grant from the EPSRC. We like to thank E Krotscheck, P Pietiläinen and A Kallio for many interesting discussions.

References

[1] Keldysh L V 1968 *Proc. 9th Int. Conf. on the Physics of Semiconductors (Moscow, 1968)* ed S M Ryvkin and V Shmastsev (Leningrad: Nauka) p 1303
[2] Ashnin V M, Rogachev A A and Sablina N I 1970 *JETP Lett.* **11** 99
[3] Pokrovsky Y E and Svitunova K I 1971 *JETP Lett.* **13** 212
[4] Dite A F, Kulakovskii V D and Timofeev V B 1977 *JETP Lett.* **45** 604
[5] Shah J, Comberscot M and Dayem A H 1977 *Phys. Rev. Lett.* **38** 1497
[6] Thomas G A, Mock J B and Capizzi M 1979 *Phys. Rev.* B **18** 4250
[7] Kulakovskii V D, Kukushkin I V and Timofeev V B 1980 *Sov. Phys.–JETP* **51** 191
[8] Smith L M and Wolfe J P 1995 *Phys. Rev.* B **51** 7521
[9] Nagai M, Shimano R and Kuwata-Gonokami M 2001 *Phys. Rev. Lett.* **86** 5795
[10] Brinkman W F and Rice T M 1973 *Phys. Rev.* B **7** 1508
[11] Beni G and Rice T M 1978 *Phys. Rev.* B **10** 768
[12] Vashishta P and Kalia R K 1982 *Phys. Rev.* B **25** 6492
[13] Feenberg E 1969 *Theory of Quantum Liquids* (New York: Academic)
[14] Krotscheck E and Saarela M 1993 *Phys. Rep.* **232** 1
[15] Apaja V *et al* 1997 *Phys. Rev.* B **55** 12925
[16] Campbell C E and Zabolitzky J G 1984 *Phys. Rev.* B **29** 123
[17] Lantto L J 1987 *Phys. Rev.* B **36** 5160

[18] Kallio A, Apaja V and Pöykkö S 1995 *Physica* B **210** 472
[19] Campbell C E 1977 *Progress in Liquid Physics* ed C A Croxton (London: Wiley) ch 6
[20] Clark J W 1979 *Progress in Particle and Nuclear Physics* (Oxford: Pergamon) vol 2, ed D H Wilkinson p 89
[21] Weisberg H and Berko S 1967 *Phys. Rev.* **154** 249
[22] Hall T M, Goland A N and Snead J C L 1974 *Phys. Rev.* B **10** 3062
[23] Arponen J and Pajanne E 1979 *Ann. Phys., NY* **121** 343
[24] Combescot M and Nozieres P 1972 *J. Phys. C: Solid State Phys.* **5** 2369